Available online at www.sciencedirect.com

ScienceDirect

Journal of Magnesium and Alloys 12 (2024) 1431–1448

www.elsevier.com/locate/jma

Full Length Article

Optimization of chemistry and process parameters for control of intermetallic formation in Mg sludges

Y. Fu[a], G.G. Wang[b,*], A. Hu[a], Y. Li[a], K.B. Thacker[b], J.P. Weiler[b], H. Hu[a,*]

[a] Department of Mechanical, Automotive and Materials Engineering, University of Windsor, 401 Sunset Ave, Windsor, Ontario N9B 3P4, Canada
[b] Global Technology Centre, Meridian Lightweight Technologies, 25 MacNab Ave, Strathroy, Ontario N7G 4H6, Canada

Received 29 November 2023; received in revised form 2 April 2024; accepted 6 April 2024
Available online 20 April 2024

Abstract

Intermetallic formation in sludge during magnesium (Mg) melting, holding and high pressure die casting practices is a very important issue. But, very often it is overlooked by academia, original equipment manufacturers (OEM), metal ingot producers and even die casters. The aim of this study was to minimize the intermetallic formation in Mg sludge via the optimization of the chemistry and process parameters. The Al_8Mn_5 intermetallic particles were identified by the microstructure analysis based on the Al and Mn ratio. The design of experiment (DOE) technique, Taguchi method, was employed to minimize the intermetallic formation in the sludge of Mg alloys with various chemical compositions of Al, Mn, Fe, and different process parameters, holding temperature and holding time. The sludge yield (SY) and intermetallic size (IS) was selected as two responses. The optimum combination of the levels in terms of minimizing the intermetallic formation were 9 wt.% Al, 0.15 wt.%Mn, 0.001 wt.% (10 ppm) Fe, 690 °C for the holding temperature and holding at 30 mins for the holding time, respectively. The best combination for smallest intermetallic size were 9 wt.% Al, 0.15 wt.%Mn, 0.001 wt.% (10 ppm) Fe, 630 °C for the holding temperature and holding at 60 mins for the holding time, respectively. Three groups of sludge factors, Chemical Sludge (CSF), Physical Sludge (PSF) and Comprehensive Sludge Factors (and CPSF) were established for prediction of sludge yields and intermetallic sizes in Al-containing Mg alloys. The CPSF with five independent variables including both chemical elements and process parameters gave high accuracy in prediction, as the prediction of the PSF with only the two processing parameters of the melt holding temperature and time showed a relatively large deviation from the experimental data. The Chemical Sludge Factor was primarily designed for small ingot producers and die casters with a limited melting and holding capacity, of which process parameters could be fixed easily. The Physical Sludge Factor could be used for mass production with a single type of Mg alloy, in which the chemistry fluctuation might be negligible. In large Mg casting suppliers with multiple melting and holding furnaces and a number of Mg alloys in production, the Comprehensive Sludge Factor should be implemented to diminish the sludge formation.

Keywords: Magnesium sludge; Al-Mn intermetallic; Optimization; Taguchi method; Sludge factor; Chemical composition; Process parameter.

1. Introduction

Sludge containing intermetallic (IM) particles is the residue settled at the bottom of the crucibles during metal melting and holding processes [1,2]. Sludge formation in Mg die casting foundry is often overlooked because it seems to be disconnected with original equipment manufacturers (OEMs), ingot producers and even design engineers of die casters. This was because the OEMs (auto companies) have dictated the Mg research fields, which are focused on the development of Mg alloys with high temperature strengths and good corrosion resistance for their own interests. Most of Mg research by academia follows the direction made by the OEMs. Meanwhile, the ingot producers and die casting companies consider the information about Mg sludge formation as their intellectual property. Therefore, there is a lack of general knowledge

* Corresponding authors.
E-mail addresses: gwang@meridian-mag.com (G.G. Wang), huh@uwindsor.ca (H. Hu).

https://doi.org/10.1016/j.jma.2024.04.011

on sludge formation mechanisms in the public domain [3]. However, sludge formation in Mg foundry is a very important topic because the improper handling of sludge could degrade product quality [4–17]. The excessive sludge formation impacts metal delivery system, contributes around 50% of total metal loss in the melting process, and acts a thermal barrier which could result in significant metal temperature fluctuation in a die casting furnace. Such metal temperature fluctuation negatively influences normal casting production from production stoppage (if metal temperature is too low) to Fe pick-up (if metal temperature is too high). Also, the magnesium melting, holding and handling practices in the casting industry showed such metal fluctuation could shorten crucible life due to thermal shock and excessive heating of the crucible steel. Therefore, it is very important to characterize Mg sludges and minimize their formation as much as possible.

The effort of minimizing the intermetallic formation in the sludges resulting from the melting and holding of Mg alloys during die casting operation was made. Thorvaldsen et al. [4] investigated the generation of sludge and dross during the melting and handling of Mg alloys, AZ91D, AM60 and AS41, in Mg die casting operations. The two main by-products of the melting and holding process were sludge and dross, sludge settled to the bottom of crucibles, while dross floated on the melt surface. The results revealed that the amount of sludge removed from the melting crucibles varied between 2 and 4% of the total metal input. It was found that intermetallic particles $Al_x(Mn)_y$ originated from Mn addition to the primary and secondary Mg ingots played an important role as precipitation sites for Fe in lowering the level of dissolved Fe and increasing the overall corrosion resistance of the castings. To establish the optimum level of Mn in Mg alloys AZ91, AM60 and AM50, Holta et al. [5] and Holta and Westengen [6] determined the temperature-dependent mutual solubility of Fe and Mn for different combination of casting temperatures and Mn additions. The analyses of sludge generated from die casting Mg alloys showed that Mn made up a much larger proportion of the AM50A sludge compared to AZ91D and AM60, because of a higher Mn content in the melt or a lower furnace temperature, encouraging the precipitation of Mn rich particles [7,8]. Sludge intermetallic generation for die casting of magnesium alloys had a direct impact on the casting product quality and operation [7]. To characterize phase constituents and contents in Mg sludge, various online and offline assessment techniques were developed [9–17]. But, almost none of them could provide rapid and accurate results simultanteously to real time control of sludge formation. To control sludge formation in aluminum alloys, a sludge factor (SF) was established, which related the chemical composition to holding temperatures of Al alloys [18–22]. With the help of the well-established Sludge Factor (SF) formula, it is relatively easy to control the sludge generation in aluminum alloys. But formation mechanisms and characteristics of sludge in die casting magnesium alloys are still unclear.

The phenomena of IM formation in various metallic materials also took place due to the change of process parameters in manufacturing processes [23–26]. Beygi et al. [23] critically reviewed the influence of alloying elements on IM formation, as aluminum alloys and steel were joined by friction stir welding (FSW). Brittle iron-rich IMs such as Fe_2Al_5 and $FeAl_3$ were found at the joint interface between Al and steel. The IM presence lowered ductility and tensile strength of the joint. Silicon in Al alloys and nickle and chromium in stainless steel retarded the growth of IM phases. During the FSW of Al (AA1050)/Mg (AZ91) alloys, a continuous IM layer of Al_3Mg_2-$Al_{12}Mg_{17}$ formed at the joint interface, through which cleavage fracture propagated as its thickness exceeded 2 µm. When the IM layer became discontinuous at the interface, the joint strength was high, and the fracture surface consisted of dimples [24]. Pouraliakbar [25] and Ghorbanzadeh [26] investigated the effect of parameters of thermomechanical processes on the IM evolution of Al-Cu-Mg alloy. Two types of IM compounds, Al_7Cu_2(Fe,Mn) and AlCuMnFeSi were identified. The composition of IM particles remained unaffected by the processing steps. The optimal aging temperature of 170 °C was obtained for the lowest volume fraction of IM particles (6.33 vol.%) concurrently with the greatest hardness, the highest thermal stability, and the lowest recrystallized fraction. In this work, a design of experiment (DOE) technique, the Taguchi method, was used to optimally control the sludge intermetallic formation in the sludge generated from the designed experimental alloys with different the chemical compositions of Al, Mn and Fe processed at various holding temperatures and times. During the optimization, the sludge yield (SY) and imtermetallic size (IS) were employed as two individual responses. The results of the response analysis were used to derive the optimal level combinations. Also, to develop the Sludge Factors (SFs) for the designed Mg alloys, multivariate linear regression analyses were carried out with the DOE results. Six Sludge Factor equations for the sludge yield and intermetallic size were established as a function of the chemical compositions and/or the processing parameters. To minimize the sludge formation, the SFs resulting in the least sludge yield and the smallest intermetallic size have to be selected for processing liquid Al-containing Mg alloys.

2. Experimental procedure

Alloy and sludge preparation. To understand the composition effect on the mechanism of sludge formation in the recycling and HPDC process, various experimental Mg alloys with different chemical compositions designed by the Taugchi method (Design of Experiment DOE) were prepared by using commercially pure Mg, Al, Mg-2 wt.% Mn and Al-10 wt.% Fe. The chemical compositions of pure Mg and Mg-Mn alloy are given in Table 1. The experimental raw metallic materials were cut in to cubes (20 mm × 20 mm × 10 mm), so that they could be easily charged into a graphite crucible. Those were melted and mixed in an electric resistance furnace to achieve the desired compositions which were verified by an Optical Emission Spectroscopy. The melt was kept at 760±10 °C for 30 min for the completion of homogenization and modification under the protective gas of Sulfur Hexaflu-

Table 1
Chemical composition of pure Mg and Mg-Mn alloy.

Materials	Element (wt.%)								
	Al	Zn	Mn	Fe	Cu	Ni	Si	Pb	Mg
Mg-2%Mn	0.0042	0.0034	1.86	0.003	0.0003	0.0005	0.0033	0.0008	Bal.
Pure Mg	0	0	0	0.0006	0	0	0.002	N/A	Bal.

oride SF_6 0.5% plus carbon dioxide (CO_2) in balance and then decreased the melt temperature to desire temperature for holding a designate period. After holding a fixed period at the desired temperature, the graphite crucible was removed from the furnace chamber, and air cooled with the cover of protective gas until the completion of solidification. The prepared samples were analyzed by inductively coupled spectrometry (ICP) to ensure an uncertainty of ±5%.

Microstructural Analysis. For the microstructure analysis of the experimental alloys, specimens were chosen and sectioned from the bottom of the air-cooled cast cylindrical sample.

The procedure of metallographic specimen preparation included sectioning, mounting, grinding, polishing.

A. Sectioning

Specimens were cut from bottom, center and top of coupons in the form of cubes with the dimensions of 10×10×10 mm.

B. Mounting

Specimens were mounted by Buehler simplimet3 mount machine. The mount materials are one of the common plastic mounting materials, cold mounting material – epoxy. Then the mounted specimens were ground down on the 180 grit by using a belt grinder to smooth the edge of the specimens.

C. Grinding

The roughly ground mounted specimens went through a wet grinding process by using the series of SiC papers in the sequence procedures: 240, 320, 400, and 600 grit.

D. Polishing

Mechanical polishing was performed in two stages by using polishing machine and DP-PAN polishing cloth with 3 μm Al_2O_3 suspension, and 0.05 μm Al_2O_3 suspension. Rough polishing (stage one) removed the major part of the disturbed metal remaining after the final grinding step. Finish polishing (stage two) removed the superficial scratches that remain after rough polishing. Then using cold water, liquid soap and ethyl alcohol cleaned the polished specimens, and dried with a hair dryer using cold air.

A Buehler (Lake Bluff, IL) optical image analyzer 2002 system was used to observe primary characteristics of the specimens. The detailed features of the microstructure were also characterized at high magnifications by a scanning electron microscope (SEM), Hitachi Tabletop Microscope TM3000, with a maximum resolution of 30 nm in a backscattered mode/1 μm in x-ray diffraction mapping mode, and useful magnification of 10 to 10,000 to maximize composition reading of the energy dispersive spectroscopy (EDS) data. The identification of the intermetallic phases was based on composition reading of the energy dispersive spectroscopy (EDS) data. A quantitative evaluation of specimen microstructures consisted of calculating area fractions of different phase constituents by using ImageJ, a public domain image processing system, to identify different microstructure constituents through image contrast.

2.1. Determination of sludge yield

Step One: Determination of density of the Al-Mn intermetallic-free alloy matrix.

1. Acquire specimens from the Al-Mn intermetallic-free zone in the cylinder casting for the density measurement of the Al-Mn intermetallic-free Mg alloy matrix;
2. Measure the density of the Al-Mn intermetallic-free Mg alloy matrix with Archimedes principle [3];

$$\rho_{alloy\ matrix} = \frac{w_a \times \rho_w}{w_a - \rho_w} \tag{1}$$

where w_a and w_w are the weights of the Al-Mn intermetallic-free specimens in air and water, respectively, ρ_w is the density of water.

Step Two: Determination of the volume fraction of the Al-Mn intermetallic in the Al-Mn intermetallic-concentrated layer.

3. Acquire specimens from the Al-Mn intermetallic-concentrated layer at the bottom of the cylinder casting for the determination of the volume fraction of the Al-Mn intermetallic;
4. Determine the volume fraction of the Al-Mn intermetallic in the Al-Mn intermetallic-concentrated layer ($V_{Al-Mn\ in\ layer}$) by image analysis (ImageJ) with the help of an optical microscope (OM) and a scanning electron microscope (SEM);

Step Three: Determination of Density of the Al-Mn intermetallic-concentrated layer.

5. Determine the volume fraction of the Mg alloy matrix ($V_{Matrix\ in\ layer}$) in the Al-Mn intermetallic-concentrated layer [11].

$$V_{Matrix\ in\ layer} = 1 - V_{Al-Mn\ in\ layer} \tag{2}$$

6. Calculate the density of the Al-Mn intermetallic-concentrated layer, which consists of (a) Al-Mn intermetallic and (b) alloy matrix, based on the Rule of Mixtures [22];

$$\rho_{layer} = \rho_{matrix\ alloy} \times V_{Matrix\ in\ layer} + \rho_{Al-Mn} \times V_{Al-Mn\ in\ layer} \tag{3}$$

where ρ_{Al-Mn} is the density of the Al-Mn intermetallic (4430 kg/m^3) [2]

Step four: Determination of the Volume of the Al-Mn intermetallic-concentrated layer

7. Measure the thickness of the Al-Mn intermetallic-concentrated layer (t_{layer}) at the bottom of the cylinder casting with an optical microscope or SEM;
8. Calculate the volume of the Al-Mn intermetallic-concentrated layer (V_{layer}) with the known diameter of the cylinder casting (d_{cs});

$$V_{layer} = \frac{1}{4}\pi d_{cs}^2 \times \ t_{layer} \tag{4}$$

Step Five: Determination of the weight of the Al-Mn intermetallic in the cylinder casting

9. Calculate the total weight of the Al-Mn intermetallic in the Al-Mn intermetallic -concentrated layer ($W_{Al-Mn\ in\ layer}$);

$$W_{Al-Mn\ in\ layer} = \rho_{Al-Mn} \ \times \ V_{Al-Mn\ in\ layer} \ \times v_{layer} \tag{5}$$

10. Determine the weight of the Al-Mn intermetallic in the entire cylinder casting ($W_{Al-Mn\ in\ cs}$), which should be equivalent to the weight of the Al-Mn intermetallic in the Al-Mn intermetallic-concentrated layer ($W_{Al-Mn\ in\ layer}$)

$$W_{\mathrm{Al-Mn\ in\ cs}} = W_{\mathrm{Al-Mn\ in\ layer}} \tag{6}$$

Step Six: Calculation of Sludge Yield

11. Calculate the sludge (Al-Mn intermetallic) yield (SY) with the following equation:

$$SY = \frac{W_{Al-Mn\ in\ cs}}{W_{cs}} \tag{7}$$

where SY is the sludge yield (%), W_{Al-Mn} is the weight of the Al-Mn intermetallic (g), and W_{cs} is the weight of the cylinder casting. Fig. 1 presents a flowchart showing the process of sludge yield determination

2.2. Determination of intermetallic size

The intermetallic size (IS) in average (D_{IS}) is calculated by [3]

$$D_{IS} = (D_l + D_s)/2 \tag{8}$$

where D_l is the longest diameter, and D_s is the shortest diameter as illustrated in Fig. 2.

2.3. Taguchi design of experiment

Design of Orthogonal Array and Signal-to-Noise Analysis. Based on the literature survey and industrial observation on Mg sludge formation, five factors of alloy chemical compositions and holding temperature and time along with four level were selected. The chosen five factors (Al, Mn, Fe and Holding Temperature and Time) with four levels were listed in Table 2. The detailed information of each factor and level employed in the orthogonal array of sixteen experiments are given in Table 3.

The intermetallic formation in liquid Mg alloys is influenced by various factors. The Taguchi method helps in identifying the significant factors affecting the intermetallic formation and optimizing the process settings to minimize their effects. In the optimization process, it is almost impossible to eliminate all errors caused by the variation of characteristics. An increase in the variance of multiple characteristics lowers the quality reliability of the process. The Taguchi method [27,28] uses the signal-to-noise (S/N) ratio instead of the average value to interpret the trial results data into a value for the characteristic evaluation in the optimum setting analysis. To minimize the influence of the error caused by the variation of characteristics, the signal-to-noise (S/N) ratio was employed, which converted the trail result data into a value for the response to evaluate the process in the optimum setting analysis. The S/N ratio consolidated several repetitions into one value which reflected the amount of variation present.

The proposition for the minimize the sludge formation, the sludge yield (SY) and intermetallic size (IS) are multiple performance characteristics (two objectives) using a weighting method is defined as the Eqs. (10)–(12) [28]:

$$\mathrm{Y_{SUM}} \ = \ \mathrm{Y_P} \times W \tag{9}$$

where

$$Y_{SUM} = \begin{bmatrix} \eta_{1c} \\ \eta_{2c} \\ \vdots \\ \eta_{9c} \end{bmatrix}, Y_p = \begin{bmatrix} \eta_{11} & \eta_{12} \\ \eta_{21} & \eta_{22} \\ \vdots & \vdots \\ \eta_{91} & \eta_{92} \end{bmatrix}, w = \begin{bmatrix} w_1 \\ \vdots \\ w_3 \end{bmatrix} \tag{10}$$

$$\sum_{i=1}^{2} w_i = 1 \tag{11}$$

where w_1 and w_2 are the weighting factor of sludge yield and intermetallic size, respectively. η_{jc} is the multi response, S/N ratio in the jth test, η_{ji} is the i_{th} single response S/N ratio

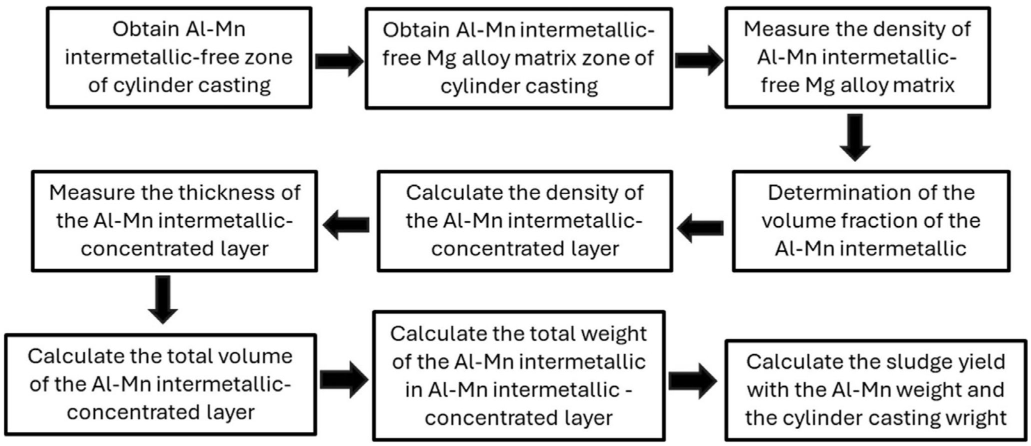

Fig. 1. Flowchart showing the process of sludge yield determination.

Table 2
Design factors and levels.

Level	Factor				
	A Al (wt.%)	B Mn (wt.%)	C Fe (wt.%)	D Holding temperature (°C)	E Holding time (Mins)
1	6	0.15	0.001	630	30
2	7	0.25	0.004	650	60
3	8	0.35	0.007	670	90
4	9	0.45	0.01	690	120

Table 3
Designed experiment plans.

Experiment	Al (%)	Mn (%)	Fe (%)	Holding temperature (°C)	Holding time (Mins)
1	6 (A1)	0.15 (B1)	0.001 (C1)	630 (D1)	30 (E1)
2	6 (A1)	0.25 (B2)	0.004 (C2)	650 (D2)	60 (E2)
3	6 (A1)	0.35 (B3)	0.007 (C3)	670 (D3)	90 (E3)
4	6 (A1)	0.45 (B4)	0.01 (C4)	690 (D4)	120 (E4)
5	7 (A2)	0.15 (B1)	0.004 (C2)	670 (D3)	120 (E4)
6	7 (A2)	0.25 (B2)	0.001 (C1)	690 (D4)	90 (E3)
7	7 (A2)	0.35 (B3)	0.01 (C4)	630 (D1)	60 (E2)
8	7 (A2)	0.45 (B4)	0.007 (C3)	650 (D2)	30 (E1)
9	8 (A3)	0.15 (B1)	0.007 (C3)	690 (D4)	60 (E2)
10	8 (A3)	0.25 (B2)	0.01 (C4)	670 (D3)	30 (E1)
11	8 (A3)	0.35 (B3)	0.001 (C1)	650 (D2)	120 (E4)
12	8 (A3)	0.45 (B4)	0.004 (C2)	630 (D1)	90 (E3)
13	9 (A4)	0.15 (B1)	0.01 (C4)	650 (D2)	90 (E3)
14	9 (A4)	0.25 (B2)	0.007 (C3)	630 (D1)	120 (E4)
15	9 (A4)	0.35 (B3)	0.004 (C2)	690 (D4)	30 (E1)
16	9 (A4)	0.45 (B4)	0.001 (C1)	670 (D3)	60 (E2)

for the jth test; w_i is the weighting factor in the i_{th} performance characteristics. The objective function was formulated according to the previous optimization criteria [28]:

$$\text{Minimize } f(X) = w_1 \cdot \eta_{\text{SY}} + w_2 \cdot \eta_{IS} \tag{12}$$

Analysis of Variance (ANOVA). The purpose of the analysis of variance is to investigate the contribution of each factor (chemical element) with multiple characteristics that significantly affect the sludge yield and intermetallic size. Following the analysis, it is relatively easy to identify the effect order of factors on the sludge yield and intermetallic size, and the contribution of factors to sludge yield and intermetallic size. In this study, variation due to both the four factors and the possible error was taken into consideration. The ANOVA was established based on the sum of the square (SS), the degree of freedom (D), the variance (V), and the percentage of the contribution to the total variation (P) [27,28].

3. Results and discussion

Determination of Optimal Levels for Sludge Yield. According to Eq. (9), two sludge yield measurements for each experiment were converted into a S/N ratio. Table 4 compares the calculated mean S/N ratios with the sludge yield data and

Table 4
The S/N ratios calculated from the determined sludge yield relevant to the experiments designed by the Taguchi method.

Experiment	Al (wt.%)	Mn (wt.%)	Fe (wt.%)	Holding temperature (°C)	Holding time (Mins)	Sludge yield (%)		
						Test 1	Test 2	S/N Ratio
1	6 (A1)	0.15 (B1)	0.001 (C1)	630 (D1)	30 (E1)	0.33	0.28	10.28
2	6 (A1)	0.25 (B2)	0.004 (C2)	650 (D2)	60 (E2)	0.45	0.46	6.84
3	6 (A1)	0.35 (B3)	0.007 (C3)	670 (D3)	90 (E3)	0.52	0.52	5.68
4	6 (A1)	0.45 (B4)	0.01 (C4)	690 (D4)	120 (E4)	0.59	0.62	4.36
5	7 (A2)	0.15 (B1)	0.004 (C2)	670 (D3)	120 (E4)	0.41	0.42	7.64
6	7 (A2)	0.25 (B2)	0.001 (C1)	690 (D4)	90 (E3)	0.43	0.45	7.13
7	7 (A2)	0.35 (B3)	0.01 (C4)	630 (D1)	60 (E2)	0.57	0.58	4.81
8	7 (A2)	0.45 (B4)	0.007 (C3)	650 (D2)	30 (E1)	0.63	0.62	4.08
9	8 (A3)	0.15 (B1)	0.007 (C3)	690 (D4)	60 (E2)	0.31	0.34	9.75
10	8 (A3)	0.25 (B2)	0.01 (C4)	670 (D3)	30 (E1)	0.46	0.46	6.74
11	8 (A3)	0.35 (B3)	0.001 (C1)	650 (D2)	120 (E4)	0.53	0.51	5.68
12	8 (A3)	0.45 (B4)	0.004 (C2)	630 (D1)	90 (E3)	0.63	0.61	4.15
13	9 (A4)	0.15 (B1)	0.01 (C4)	650 (D2)	90 (E3)	0.32	0.33	9.76
14	9 (A4)	0.25 (B2)	0.007 (C3)	630 (D1)	120 (E4)	0.42	0.41	7.64
15	9 (A4)	0.35 (B3)	0.004 (C2)	690 (D4)	30 (E1)	0.51	0.53	5.68
16	9 (A4)	0.45 (B4)	0.001 (C1)	670 (D3)	60 (E2)	0.61	0.62	4.22

Table 5
The mean factor response of sludge yield.

Levels	Al (%)	Mn (%)	Fe (%)	Holding temperature (°C)	Holding time (Mins)
1	6.79	9.36	6.83	6.72	6.70
2	5.91	7.09	6.42	6.07	6.41
3	6.58	5.46	6.79	6.59	6.68
4	6.83	4.20	6.08	6.73	6.33

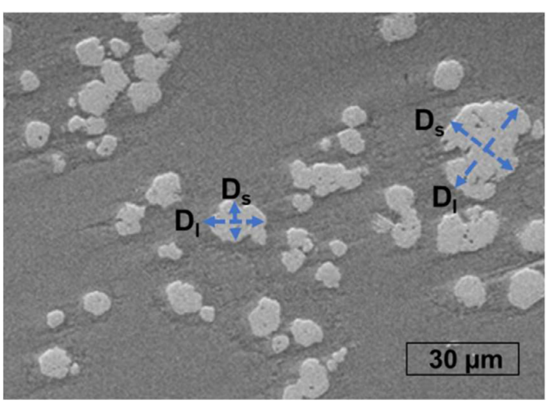

Fig. 2. SEM micrographs illustrating the definition of the longest diameter (D_l) and the shortest diameter (D_s) for calculation of the average size of the intermetallic phase (D_{IS}).

level numbers. In the following discussion, the S/N ratios were employed as a response index to compare the sludge yields of the different designed alloys and casting parameters instead of directly using the values of the sludge yield. The response of each factor to its individual level was calculated by averaging the S/N ratios of all experiments at each level for each factor. The determined factor responses are summarized in Table 5. Fig. 3 shows the effect of the five factors, Al, Mn, Fe, Holding Temperature and Holding Time on the mean S/N ratios, and single response signal-to-noise graph for case the only considering only the sludge yield.

Fig. 3(a) shows the response of the S/N ratio to Al content. It can be seen from Fig. 3(a) that the mean S/N ratio dropped to the bottom of the curve as the Al content increase to 7% (level 2) from 6% (level 1). When the Al content kept increasing to 8% (level 3), the mean S/N ratio bounced back upward. The upward tendency was kept further rising to 9% (level 4), which gave the highest value of mean S/N ratio. The observation on the response of the S/N ratio to the Al content might be mainly due to the variation of Mn content. Since both Mn and Fe were almost insoluble in liquid magnesium and instead reacted with Al solute to form Al-Mn-Fe intermetallic. It was observed that an increase in Al content resulted in the generation of more Al-Mn-Fe intermetallics due to the Mn demand. However, further extending the Al content, if the Al content over the Mn saturation point, the additional Al could react with Mg to form $Mg_{17}Al_{12}$ intermetallic phase during solidification.

The response of the S/N ratio to Mn content is shown in Fig. 3(b). The mean S/N ratio demonstrated an almost linearly decrease tendency from 0.15% (level 1) to 0.45% (level 4). This might result from the high affecting of the Mn with Al and impurity Fe, to form Al-(Mn,Fe) intermetallics for Fe eliminate at high temperature over 700 °C in liquid Mg. In the production of Mg alloys, sufficient Mn is usually added to ensure that the Fe:Mn ratio is less than 0.032, which substantially improves the corrosion resistance [25,26]. As a result, the rich Mn content in Mg alloy promoted the formation of the intermetallic in the sludge.

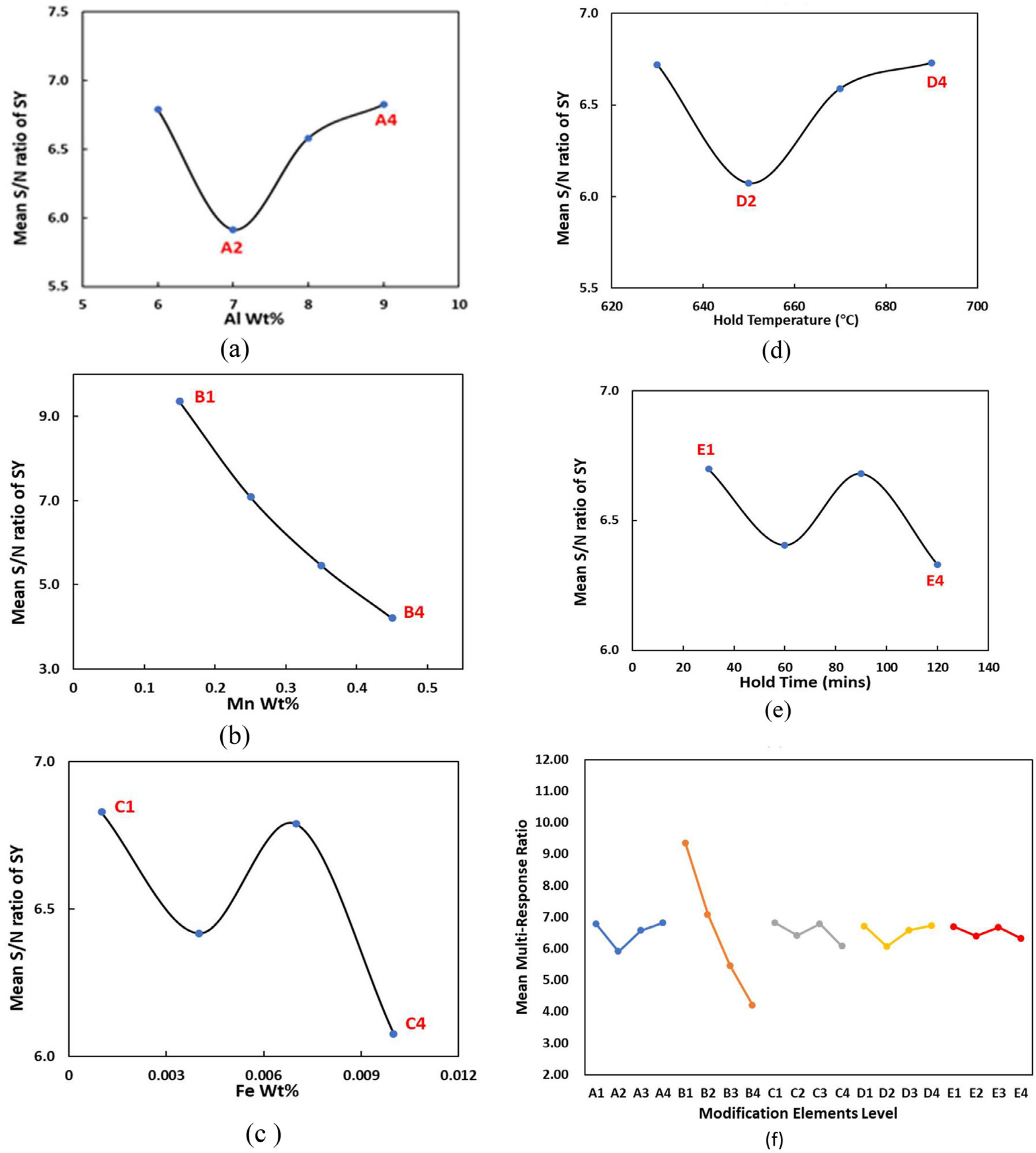

Fig. 3. Effects of (a) Al, (b) Mn, (c) Fe contents, (d) holding temperature and (e) holding time on the mean S/N ratio, and (f) single response signal-to-noise graph for case the only considering only the sludge yield.

Fig. 3(c) shows response of the S/N ratio to the Fe content. The mean S/N ratio decreased at first as the Fe content increased from 10 ppm (level 1) to 40 ppm (level 2). Then, the S/N ratio rose, while the Fe content became to 70 ppm (level 3). Lastly, the S/N ratio decreased to the lowest value as the Fe content increased to 100 ppm (level 4). The purpose of introducing additional iron up to 100 ppm to the alloys was to simulate the iron picking process in the steel crucible used in the industry, since the Fe-free high-quality graphite crucible was employed in this study. At high temperatures, with inappropriate manganese content, magnesium and the alloying elements could react with the steel crucible. The variation of S/N ratio with the Fe content could be caused by the different Fe/Mn ratio. It was reported that the proper control of the manganese and iron ratio was the essential role for sludge formation [26].

Fig. 3(d) shows the response of the S/N ratio to the holding temperature parameter similar to that for the Al content. The mean S/N ratio decreased at first as the holding temperature increased from 630 °C (level 1) to 650 °C (level 2). The S/N ratio then increased to its highest value as the holding temperature parameter increased to 690 °C (level 4). At 650 °C (level 2), the lowest S/N ratio was produced. it was might be due to the precipitation of the Al_8Mn_5 intermetallic

Table 6
Results of the ANOVA for sludge yield.

Factors	Degree of freedom (D)	Sum of squares (SSp)	Variance (V)	Corrected sums of squares (SSp')	Contribution	Rank
Al (%)	3	2.15	0.72	2.15	3.32%	2
Mn (%)	3	59.47	19.82	59.47	91.91%	1
Fe (%)	3	1.43	0.48	1.43	2.22%	3
Holding temperature (°C)	3	1.22	0.41	1.22	1.88%	4
Holding time (Mins)	3	0.43	0.14	0.43	0.66%	5
Error		0.00	0.00		0	
Total		6.286			100%	

phase took place at 642 °C by thermal analysis with differential scanning calorimetry (DSC) measurements which was report by Thorvaldsen et al. [4]. The high S/N ratio at 690 °C suggested that there might be a low tendency of intermetallic precipitation at a high temperature. At a relatively low temperature of 630 °C, the high viscosity and poor fluidity could result in low precipitation of intermetallic in Mg sludge.

Fig. 3(e) presents the response of the S/N ratio to the holding time parameter, which was similar to that for the iron content. The mean S/N ratio decreased at first as the holding time increased from 30 min (level 1) to 60 mins (level 2). Then, the S/N ratio increased when the holding time increased to 90 mins (level 3). Lastly, the S/N ratio decreased to the lowest value as the holding time rose to 120 mins (level 4). Although there were no specific holding times used in the foundry report, the adoption of the holding times in this study was based on down time experienced in the Mg casting operation. The result of the S/N ratio indicated the long holding time encouraged the intermetallic formation in the Mg sludge.

By selecting the highest value of mean S/N ratio for each factor, the optimal level was determined. On this basis, the optimum combination of the levels in terms of minimizing the intermetallic formation of the designed alloy was A4B1C1D4E1 as shown in Fig. 3(f). They were 9 wt.% Al, 0.15 wt.%Mn, 0.001 wt.% (10 ppm) Fe, 690 °C for holding temperature and holding at 30 mins respectively. In contrast, the most sludge yield combination of designed alloy was A2B4C4D2E4, which were 7 wt.%Al, 0.45 wt.%Mn, 0.01 wt.% (100 ppm) Fe, 650 °C for holding temperature and 120mins for holding time.

Factor Contributions. The contribution of each factor to the sludge yield was determined by performing the analysis of variance based on Eqs. (14)–(18). The results of the analysis of variance (ANOVA) and contribution of the five factors are summarized in Table 6. The contribution of the five factors, the Al content, Fe content, holding temperature and holding time was 3.32%, 2.22%, 1.88% and 0.66%, respectively. The contribution of Mn content (91.91%) was significantly higher than the sum (8.08%) of the contributions of all the other four factors. It was evident that, among the selected factors, the Mn content had the major influence on the intermetallic formation. Furthermore, it could be assumed that the Al, Fe, holding temperature and holding time have almost the same effect on intermetallic formation in the sludge because of the minor difference in the contribution percentages among these four factors.

It was evident from Table 6 that the ANOVA analysis not only specified how important a factor was to the intermetallic formation by numbers but also showed their relative effect. By ranking their relative contributions, the sequence of the five factors affecting the intermetallic formation was the Mn, Al, Fe contents and the holding temperature and holding time. It is also worthwhile mentioning that, in the ANOVA analysis, if the percentage error (P_e) contribution to the total variance is lower than 15%, no important factor is missing in the experimental design. In contrast, if the percent contribution of the error exceeds 50%, certain significant factors are overlooked and the experiments must be re-designed. As shown in Table 6, the percentage error (P_e) was 0%. This indicated that no significant factors were missing in the experimental design.

Confirmation Experiment. The confirmation experiment was the final step in verifying the conclusions from the previous round of experimentation. If the results of the confirmation runs are not consistent with the expected conclusions, a new Taguchi method design is required. The least sludge yield confirmation experiment was performed by setting the experimental condition of the five factors as: 9%Al, 0.15%Mn, 0.001%Fe and 690 °C for the holding temperature and 30 min for the holding time. The levels of the corresponding factors for the most sludge yield confirmation was 7 wt.%Al, 0.45 wt.%Mn, 0.01 wt.%Fe, 650 °C for holding temperature and 120mins for holding time. Fig. 4 presents the SEM micrographs showing the Al-Mn intermetallic-free zone and the Al-Mn intermetallic-concentrated layer of the confirmation alloy with the least sludge. The EDS spectra given in Fig. 5 revealed that two phases, α-Mg matrix (dark), and Mn-containing intermetallic phases (gray) were present in the test alloy. The element analysis showed that there were 93.21 at.% Mg and 6.79 at.% Al in the α-Mg matrix. The Mn-containing intermetallic phase contained 41.91 at.% Mg, 35.78 at.% Al, 20.36 at.% Mn and 1.95 at.% Fe. The ratios around 1.77 between Al and Mn suggested that the Mn-containing intermetallic particles could be considered as Al_8Mn_5 phase, which was reported in references 1, 2 and 3. The thickness of the sludge concentrated layer for least sludge yield confirmation was 0.5 mm, which was the least of thin thickness in this study. Based on the measured layer thickness, the sludge yield of 0.26 was calculated by Eqs. (1)–(7), which was the lowest

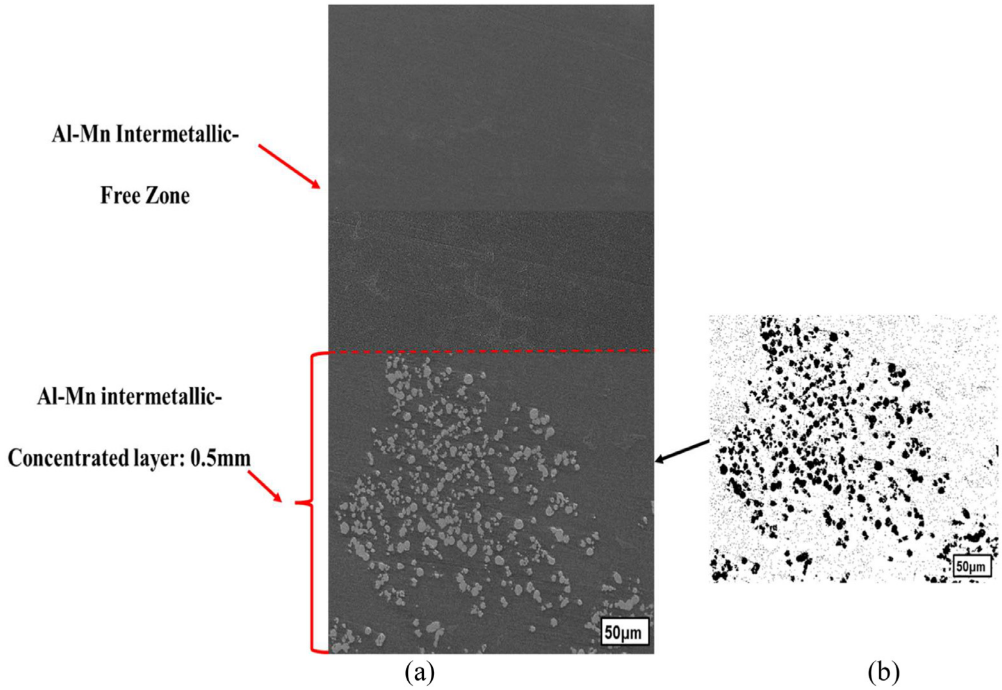

Fig. 4. (a) SEM micrograph illustrating the Al-Mn intermetallic-free zone and the Al-Mn intermetallic-concentrated layer, (b) binary black and white image from ImageJ showing the intermetallic contents of the alloy with the least sludge yield from the confirmation experiment.

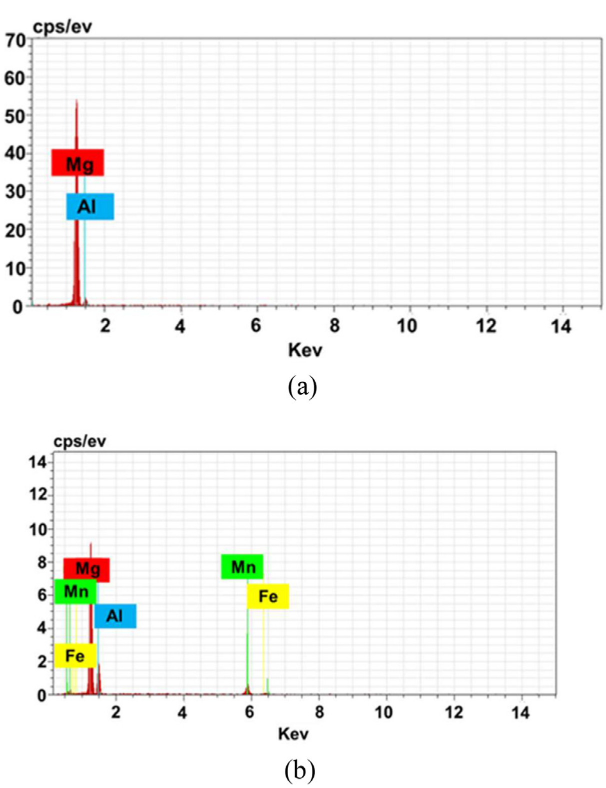

Fig. 5. EDS spectra (a) and (b) for the areas containing α-Mg matrix (dark), and Mn-containing intermetallic phases (gray) as shown in Fig. 8(a), respectively.

yield obtained in the present study. The Al-Mn intermetallic zone and the Al-Mn intermetallic-concentrate layer of the confirmation alloy with the most sludge yield was revealed in Fig. 6, the measured thickness of the Al-Mn intermetallic-concentrated layer for the most sludge yield confirmation was 1 mm, the subsequently calculated sludge yield was 0.65, which was the highest value of the sludge yield in this study.

Summary for Sludge Yield. The Taguchi method for the design of experiment was used for minimizing the Al-Mn intermetallic formation in the sludge during the Mg alloy die casting process. The Mn content was found to be the major factor affecting the sludge formation, while Al content, Fe content, holding temperature and holding time have a similar contribution, but smaller effect on the sludge production. The contribution Al content, Mn content, Fe content, holding temperature and holding time were 3.32%, 91.91%, 2.22%, 1.88% and 0.66%, respectively. The least sludge yield combination was 9%Al, 0.15%Mn, 0.001%Fe and 690 °C for holding temperature and 30 min holding time and the most sludge yield combination were 7%Al, 0.45%Mn, 0.01%Fe, 650 °C for holding temperature and 120mins for holding time.

Determination of Optimal Levels for Intermetallic Size. Base on the Eq. (9), two measurements of the intermetallic size (IS) for each experiment were converted into a S/N ratio. Table 7 compares the calculated mean S/N ratios with the IS data and level numbers. The determined factor responses are summarized in Table 8. Fig. 7 shows the effect of the five factors, Al, Mn, Fe, holding Temperature and holding time on the mean S/N ratios, respectively.

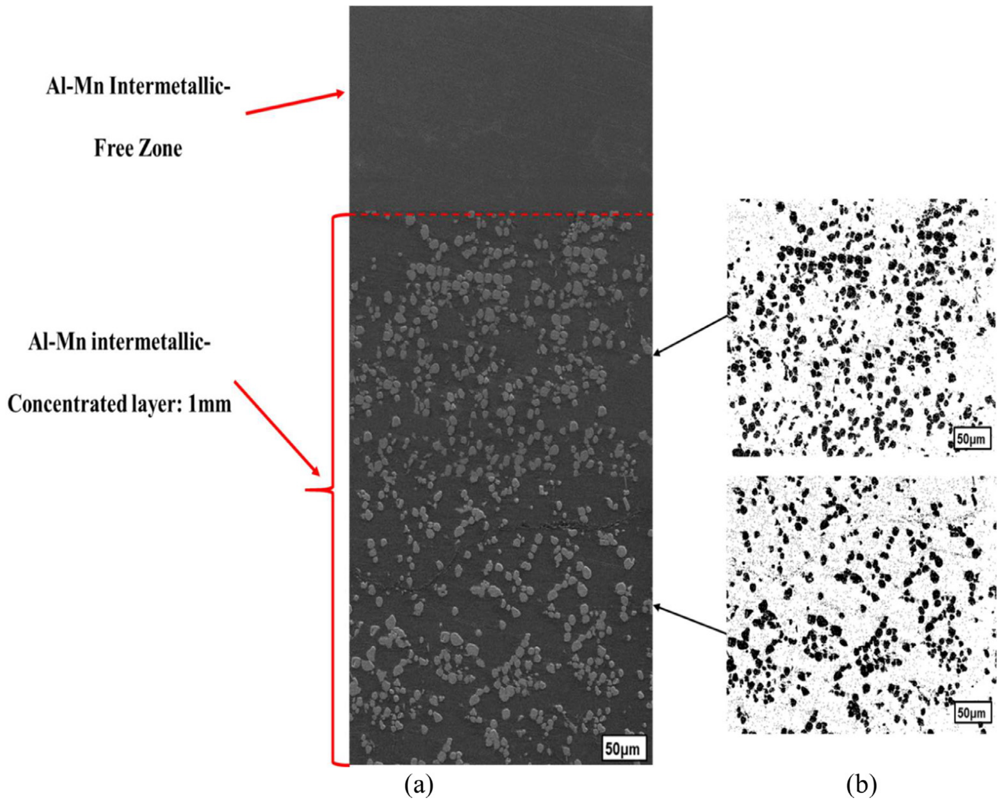

Fig. 6. (a) SEM micrograph illustrating the Al-Mn intermetallic-free zone and the Al-Mn intermetallic-concentrated layer, (b) binary black and white images from ImageJ showing the intermetallic contents of the alloy with the most sludge yield from the confirmation experiment.

Table 7
The S/N ratios calculated from the determined intermetallic size relevant to the experiments designed by the Taguchi method.

Experiment	Al (wt.%)	Mn (wt.%)	Fe (wt.%)	Holding temperature (°C)	Holding time (Mins)	Intermetallic size (μm)		
						Test 1	Test 2	S/N ratio
1	6 (A1)	0.15 (B1)	0.001 (C1)	630 (D1)	30 (E1)	11.54	10.5	−20.48
2	6 (A1)	0.25 (B2)	0.004 (C2)	650 (D2)	60 (E2)	13.09	13.23	−22.39
3	6 (A1)	0.35 (B3)	0.007 (C3)	670 (D3)	90 (E3)	14.81	14.64	−23.36
4	6 (A1)	0.45 (B4)	0.01 (C4)	690 (D4)	120 (E4)	16.43	15.9	−24.17
5	7 (A2)	0.15 (B1)	0.004 (C2)	670 (D3)	120 (E4)	18.02	12.2	−24.07
6	7 (A2)	0.25 (B2)	0.001 (C1)	690 (D4)	90 (E3)	17.4	14.91	−24.19
7	7 (A2)	0.35 (B3)	0.01 (C4)	630 (D1)	60 (E2)	11.03	15.06	−22.41
8	7 (A2)	0.45 (B4)	0.007 (C3)	650 (D2)	30 (E1)	17.58	17.28	−24.83
9	8 (A3)	0.15 (B1)	0.007 (C3)	690 (D4)	60 (E2)	12.43	12.49	−21.91
10	8 (A3)	0.25 (B2)	0.01 (C4)	670 (D3)	30 (E1)	17.2	17.01	−24.66
11	8 (A3)	0.35 (B3)	0.001 (C1)	650 (D2)	120 (E4)	15.01	16.05	−23.83
12	8 (A3)	0.45 (B4)	0.004 (C2)	630 (D1)	90 (E3)	15.58	13.55	−23.29
13	9 (A4)	0.15 (B1)	0.01 (C4)	650 (D2)	90 (E3)	13.04	12.33	−22.07
14	9 (A4)	0.25 (B2)	0.007 (C3)	630 (D1)	120 (E4)	12.04	12.13	−21.64
15	9 (A4)	0.35 (B3)	0.004 (C2)	690 (D4)	30 (E1)	14.78	11.79	−22.52
16	9 (A4)	0.45 (B4)	0.001 (C1)	670 (D3)	60 (E2)	14.56	14.2	−23.16

Table 8
The factor response of intermetallic size.

Levels	Al (%)	Mn (%)	Fe (%)	Holding temperature (°C)	Holding time (Mins)
1	−22.60	−22.13	−22.91	−21.96	−23.12
2	−23.87	−23.22	−23.07	−23.28	−22.47
3	−23.42	−23.03	−22.94	−23.81	−23.23
4	−22.35	−23.86	−23.33	−23.20	−23.43

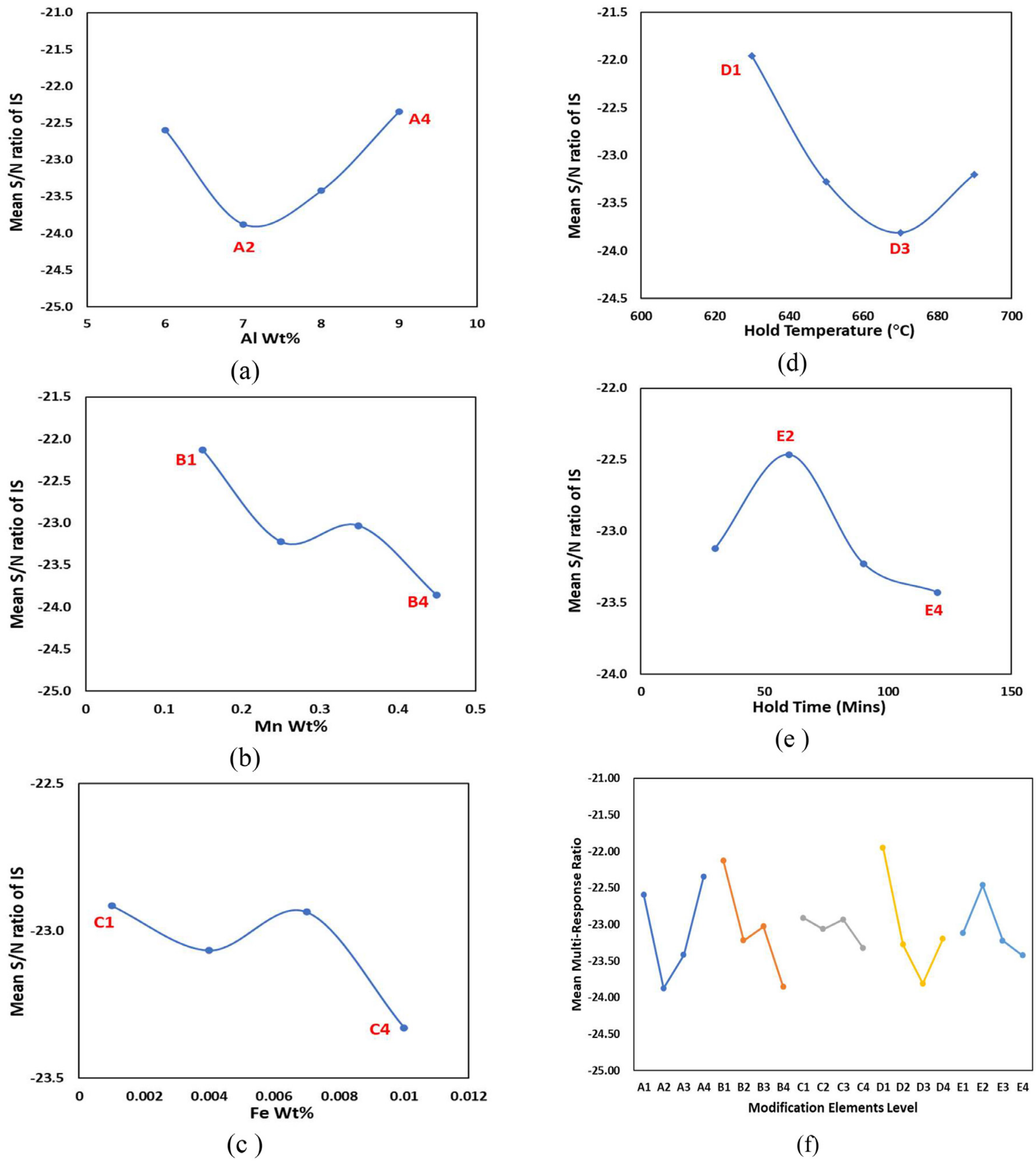

Fig. 7. Effects of (a) Al, (b) Mn, (c) Fe contents, (d) holding temperature and (e) holding time on the mean S/N ratio, and (f) single response signal-to-noise graph for case only consider intermetallic size.

Fig. 7(a) shows the response of the S/N ratio to Al content. It can be seen from Fig. 7(a) that the mean S/N ratio dropped to the bottom of the curve as the Al content increased to 7% (level 2) from 6% (level 1). When the Al content keeps increasing to 8% (level 3), the mean S/N ratio bounced back upward. The upward tendency kept further rising to 9% (level 4), which showed the highest value of mean S/N ratio. The observation on the response of the S/N ratio to Al content might be mainly due to the variation of Mn content and the holding temperature. Since both Mn and Fe were almost insoluble in liquid Mg, and instead reacted with Al solute to form Al-Mn-Fe intermetallic. It was observed that the increase in Al content results in the generation large size intermetallic due to the Mn demand and holding temperature. However, further extending the Al content, if the Al content over the Mn saturation point, the additional Al reacted with α-Mg to form $Mg_{17}Al_{12}$ intermetallic phase during solidification.

The response of the S/N ratio to Mn content is shown in Fig. 7(b). The mean S/N ratio demonstrated a decrease tendency from 0.15% (level 1) to 0.25% (level 2), the mean response S/N ratio of the IS decreased from −22.13 to −23.22. The ratio showed almost no increase to −23.03 (+0.8%) when Mn rose to 0.35% (level 3). Then S/N ratio decreased to lowest as the Mn increased to 0.45% (level 4). This might result from the variation of the Mn amount reacting with Al and impurity Fe for elimination Fe. In the Mg alloy production, sufficient Mn is usually added to ensure that the Fe:Mn ratio is less than 0.032 which substantially improves the corrosion resistance [25,26]. The variation of S/N ratio with the Fe content could be caused by the different Fe/Mn ratio. It was reported that the proper control of the manganese and iron ratio was the essential role for intermetallic size [26].

Fig. 7(c) shows response of the S/N ratio to the Fe content. The mean S/N ratio showed almost no difference from 10 ppm (level 1) to 70 ppm (level 3), since the ratio from level 1 to level 2 only decreased 0.70%, and from level 2 to level 3, only increased 0.56%. As the Fe increased to 100 ppm (level 4), the S/N ratio decreased to the lowest value. The purpose to add additional iron content to the alloy was to simulate the iron picking process in the steel crucible, as the Fe-free high-quality graphite crucible was employed in this study. At high temperatures, could with inappropriate manganese content, magnesium and the alloying elements can react with the steel crucible. Changes in the melt temperature led to intermetallic cluster. Therefore, the manganese and iron ratio were the essential role for intermetallic cluster and it was also proof the fluctuation S/N ratio with the iron content increase.

Fig. 7(d) shows the response of the S/N ratio to the holding temperature parameter similar to that for the Al content. The mean S/N ratio continuously decreased from −21.96 to −23.81 since the holding temperature increased from 630 °C (level 1) to 670 °C (level 3). However, after level 3 the S/N bounced up to −23.20 with the holding temperature up to 690 °C (level 4). Since 630 °C (level 1) was the highest S/N ratio that intend intermetallic may not cluster easily. it might be due to the 630 °C just over the commercial Mg alloy liquids temperature and molten had poor fluidity. But the intermetallic was not well-precipitation at 690 °C (level 4).

Fig. 7(e) presents the response of the S/N ratio to the holding time parameter. The mean S/N ratio increased to peak at first as the holding time increased from 30 mins (level 1) to 60 mins (level 2). Then the S/N ratio decreased through the holding time increased to 90 mins (level 3). Lastly, the S/N ratio decreased to the lowest value as the holding time increased to 120 (level 4). Although there were no specific holding times used in the foundry report, the adoption of the holding time in this study was based on down time experienced in the Mg casting operation. The result of the S/N ratios indicated the long holding time encouraged the intermetallic cluster.

By selecting the highest value of mean S/N ratio for each factor, the optimal level was determined. On this basis, the optimum combination of the levels in terms of minimizing the IS of the designed alloy the smallest IS was A4B1C1D1E2 as shown in Fig. 7(f), which were 9 wt.% Al, 0.15 wt.% Mn, 0.001 wt.% (10 ppm) Fe, 630 °C for holding temperature and holding at 60 mins. In contrast, the largest intermetallic size combination of designed alloy was A2B4C4D3E4 which were 7 wt.% Al, 0.45 wt.% Mn, 0.01 wt.% (100 ppm) Fe, 670 °C for holding temperature and 120 mins for holding time.

Factor Contributions. The results of the analysis of variance (ANOVA) and contribution of the five factors are summarized in Table 9. The contribution of five factor Al content, Mn content, Fe content, holding temperature and holding time was 27.41%, 27.65%, 1.97%, 33.52% and 9.44% respectively. It was evident that, among the selected factors, the holding temperature parameter had the highest contribution of 33.52% on the IS. Mn (27.65%) and Al (27.41%) were ranked as the second and third highest contributors which were a very close contribution to each other. The holding time and Fe content were the lowest two least contributors which were 9.44% and 1.97%, respectively.

It is also worthwhile mentioning that, in the ANOVA analysis, if the percentage error (P_e) contribution to the total variance is lower than 15%, no important factor is missing in the experimental design. In contrast, if the percent contribution of the error exceeds 50%, certain significant factors are overlooked and the experiments must be re-designed. As shown in Table 9, the percentage error (P_e) was 0%. This indicates that no significant factors were missing in the experimental design.

Confirmation Experiment. The confirmation experiment was the final step in verifying the conclusions from the previous round of experimentation. If the results of the confirmation runs are not consistent with the expected conclusions, a new Taguchi method design is required. The least intermetallic size confirmation experiment was performed by setting the experimental condition of the five factors as: 9%Al, 0.15%Mn, 0.001%Fe and 630 °C for the holding temperature and 60 min for the holding time. The levels of the corresponding factors for the most intermetallic size confirmation were 7 wt.%Al, 0.45 wt.%Mn, 0.01 wt.%Fe, 670 °C for holding temperature and 120 mins for holding time. Fig. 8 presents the SEM micrographs showing the Al-Mn intermetallic-free zone and the Al-Mn intermetallic-concentrated layer of the confirmation alloy with the least intermetallic size. The size of the sludge concentrated layer for least intermetallic size confirmation was 10.01 μm, which was the least of intermetallic size in this study. The Al-Mn intermetallic zone and the Al-Mn intermetallic-concentrate layer of the confirmation alloy with the most intermetallic size was revealed in Fig. 9, the measured size of the Al-Mn intermetallic- concentrated layer for the most intermetallic size confirmation was 18.11 μm, which was the highest value of the sludge yield in this study.

Summary for Intermetallic Size. The Taguchi method for the design of experiment was used for minimizing the IS during the Mg alloy die casting process. The contribution Al content, Mn content, Fe content, holding temperature and holding time are 27.41%, 27.65%, 1.97%, 33.52% and 9.44%, respectively. The holding temperature was found to be the most significant factor affecting the IS, while Mn content, Al content, holding time and Fe content were ranked the second to fifth. For the smallest IS combination of the optimum levels and factor was 9 wt.%Al, 0.15 wt.%Mn, 0.001 wt.%Fe and 630 °C for the holding temperature and 60 min for the holding time. For the largest IS combination was 7 wt.%Al,

Table 9
Results of the ANOVA for intermetallic size.

Factors	Degree of freedom (D)	Sum of squares (SSp)	Variance (V)	Corrected sums of squares (SSp')	Contribution	Rank
Al (%)	3	6.06	2.02	6.06	27.41%	3
Mn (%)	3	6.11	2.04	6.11	27.65%	2
Fe (%)	3	0.44	0.15	0.44	1.97%	5
Holding temperature (°C)	3	7.41	2.47	7.41	33.52%	1
Holding time (Mins)	3	2.09	0.70	2.09	9.44%	4
Error		0.00	0.00		0	
Total		6.286			100%	

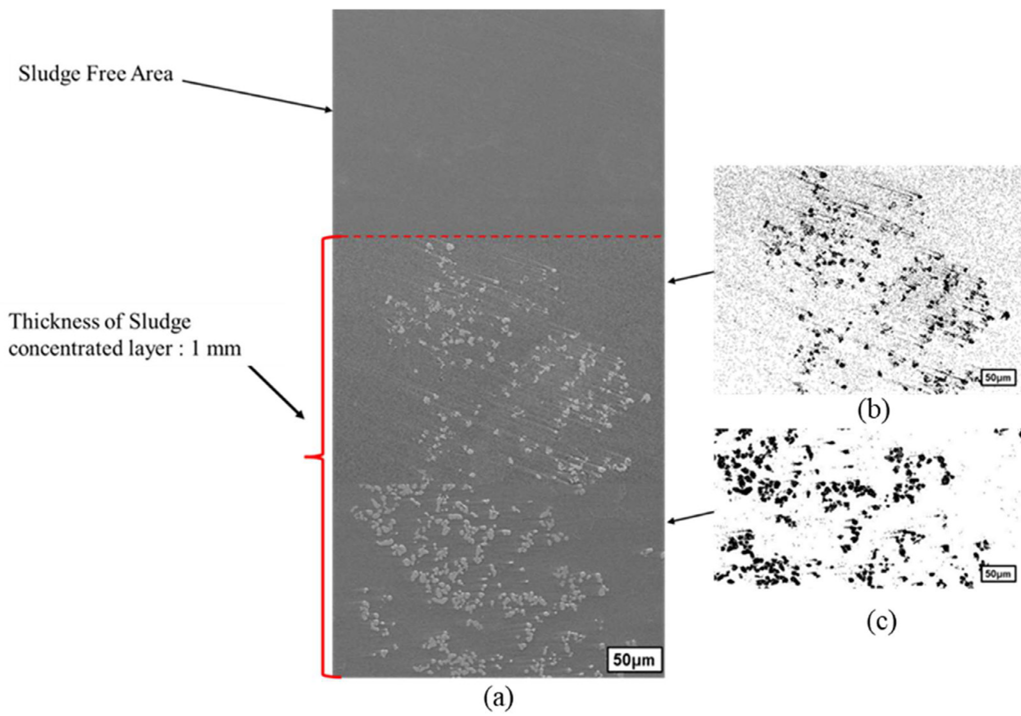

Fig. 8. (a) SEM micrograph illustrating the Al-Mn intermetallic-free zone and the Al-Mn intermetallic-concentrated layer, (b) and (c) binary black and white images from ImageJ showing the intermetallic contents of the alloy with the least intermetallic size from the confirmation experiment.

0.45 wt.%Mn, 0.01 wt.%Fe, 670 °C for the holding temperature and 120 mins for the holding time.

As an ongoing research project, a further investigation into detailed microstructure characteristics such as phase identification by transmission electron microscopy (TEM) and aggregation of intermetallic particles by X-ray computed tomography are to be performed, and the results are to be published in the near future.

Chemical, Process and Comprehensive Sludge Factors for Al-containing Mg Alloys. For casting Al alloys, the formulae, named Sludge Factor (SF), as a function of the chemical composition and/or melt holding temperature were established, which enabled the control of sludge formation [18–22]. To develop a Sludge Factor for Mg alloys, multivariate linear regression analyses were carried out with the DOE results. Since either chemical compositions or processing parameters played an important role in sludge formation in terms of their yield intermetallic sizes. Three groups of the SFs were categorized. The first group contained the Chemical Sludge Factors (CSF) only dependent on the chemical compositions, i.e., Al, Mn and Fe contents, while the Sludge Factors in group two were influenced by the processing parameters of the melt holding temperature and time, named Process Sludge Factor (PSF). Group three possessed the SFs determined by both the chemical compositions and the processing parameters, called Comprehensive Sludge Factor (CPSF). In each group, two types of the SFs, were defined based on the output results of the DOE, i.e., sludge yield and intermetallic size.

The Chemical Sludge Factor was primarily designed for small ingot producers and die casters with a limited melting and holding capacity, of which process parameters could be fixed easily. The Physical Sludge Factor could be used for mass production with a single type of Mg alloy, in which the chemistry fluctuation might be negligible. In large Mg casting suppliers with multiple melting and holding furnaces and a number of Mg alloys in production, the Comprehensive Sludge Factor should be implemented to diminish the sludge formation. To minimize sludge formation, avoid sludge

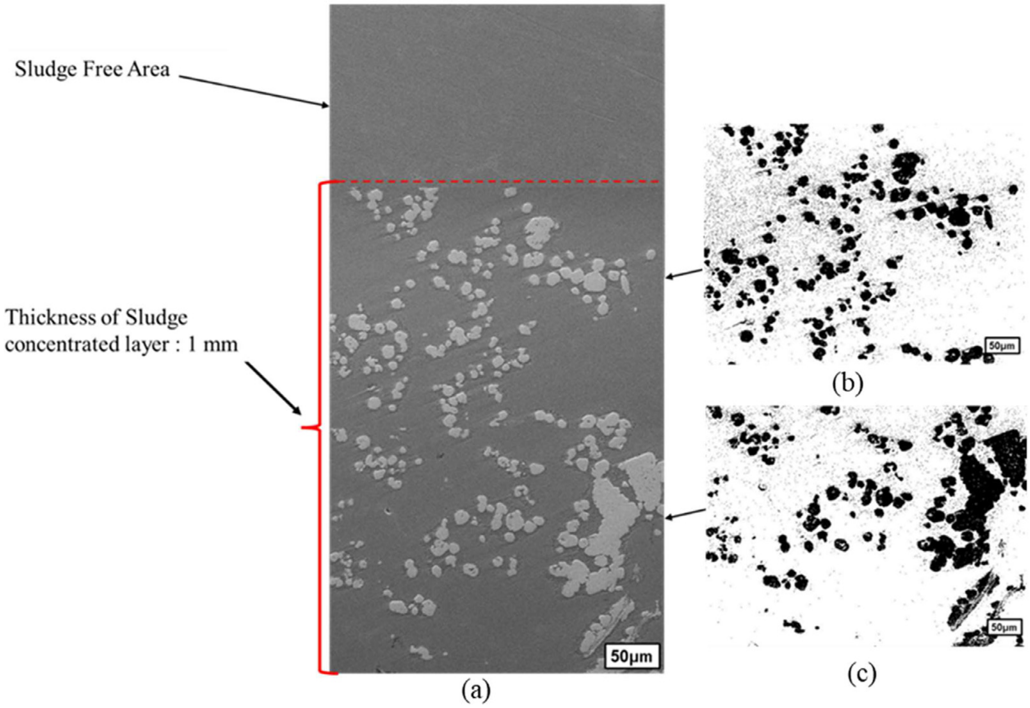

Fig. 9. (a) SEM micrograph illustrating the Al-Mn intermetallic-free zone and the Al-Mn intermetallic-concentrated layer, (b) and (c) binary black and white images from ImageJ showing the intermetallic contents of the alloy with the most intermetallic size from the confirmation experiment.

buildup in holding crucibles, address hard spots in cast components, and improve the fluidity of liquid metal in die-casting processes, it is suggested that, based on the obtained results, the calculated SF values should be less than 0.3% for the sludge yield and 10 μm for intermetallic size, respectively.

In Group One, the regression analyses [29] gave the CSFs as follows:

$$CSF^{SY}(wt.\%) = 2.11 \times 10^{-2} \times (wt.\%\ Al) + 1.01 \times (wt.\%\ Mn) + 3.13 \times (wt.\%\ Fe) \quad (13)$$

where CSF^{SY} was Chemical Sludge Factor for the sludge yield, and the regression coefficient R^2 was 0.9932 with standard error $S = 0.0451$;

$$CSF^{IS}(\mu m) = 1.12 \times (wt.\%\ Al) + 13.66 \times (wt.\%\ Mn) + 177.07 \times (wt.\%\ Fe) \quad (14)$$

where CSFIS was Chemical Sludge Factor for the intermetallic size, the regression coefficient R2 was 0.9720 with standard error $S = 2.6769$.

In Group Two, the regression analyses [29] provided the PSFs below:

$$PSF^{SY}(wt.\%) = 7.21 \times 10^{-4} \times T + 9.41 \times 10^{-5} \times t \quad (15)$$

where PSF^{SY} was Process Sludge Factor for the sludge yield, T was the temperature (°C), t was the time (minute), and the regression coefficient R^2 was 0.9536 with standard error $S = 0.1140$;

$$PSF^{IS}(\mu m) = 2.10 \times 10^{-2} \times T + 6.24 \times 10^{-3} \times t \quad (16)$$

where PSF^{IS} was Process Sludge Factor for the intermetallic size, T was the temperature (°C), t was the time (minute), and the regression coefficient R^2 was 0.9854 with standard error $S = 1.8651$.

In Group Three, the regression analyses [29] showed the CPSFs as follows:

$$CPSF^{SY}(wt.\%) = -2.57 \times 10^{-3} \times (wt.\%\ Al) + 9.18 \times 10^{-1} \times (wt.\%\ Mn) + 1.20 \times (wt.\%\ Fe) + 3.26 \times 10^{-4} \times T + 7.42 \times 10^{-5} \times t \quad (17)$$

where $CPSF^{SY}$ was Comprehensive Sludge Factor for the sludge yield, and the regression coefficient R^2 was 0.9971 with standard error $S = 0.0324$;

$$CPSF^{IS}(\mu m) = -2.83 \times 10^{-1} \times (wt.\%\ Al) + 7.73 \times (wt.\%\ Mn) + 56.23 \times (wt.\%\ Fe) + 2.02 \times 10^{-2} \times T + 6.21 \times 10^{-3} \times t \quad (18)$$

where $CPSF^{IS}$ was Comprehensive Sludge Factor for the intermetallic size, the regression coefficient R^2 was 0.9896 with standard error $S = 1.7724$.

In statistics, the value of the regression coefficients R^2 is an indicator of how well the equation (model) resulting from the regression analysis explains the relationship among the variables. As a statistical measure of fit, it indicates how much variation of a dependent variable is explained by the independent variable(s) in a regression model [29]. Although high R-squared values are good, they do not show how far the data points are from the regression line. High R-squared values are needed for models to produce precise predictions. It is impossible to use R-squared to evaluate the precision

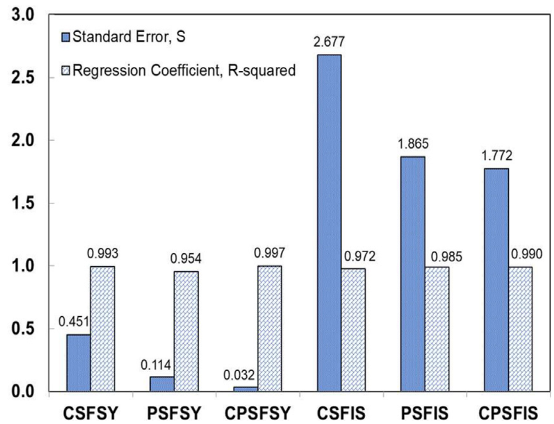

Fig. 10. Regression coefficients R^2 with standard errors for six developed SFs. CSFSY, PSFSY, CPSFSY, CSFIS, PSFIS, and CPSFIS stand for the sludge factors of CSF^{SY}, PSF^{SY}, $CPSF^{SY}$, CSF^{IS}, PSF^{IS}, and $CPSF^{IS}$, respectively.

of the predictions. But, the standard error of the regression provides the absolute measure of the typical distance that the data points fall from the regression line, which measures the precision of the model's predictions [29]. Fig. 10 presents the regression coefficients R^2 with the standard errors for six developed SFs, i.e., CSF^{SY}, PSF^{SY}, $CPSF^{SY}$, CSF^{IS}, PSF^{IS}, and $CPSF^{IS}$. All the regression coefficients R^2 for six developed SFs had a relatively high value above 0.95, indicating that the measured data points were closer to the fitted values. Examination of the standard errors revealed that the SFs for the sludge yield, i.e., 0.0451 for CSF^{SY}, 0.1140 for PSF^{SY}, and 0.0324 for $CPSF^{SY}$, had lower S values than those for the intermetallic size, i.e., 2.6769 for CSF^{IS}, 1.8651 for PSF^{IS}, 1.7724 for $CPSF^{IS}$, respectively. The standard error analyses indicated that the SFs for the sludge yield could generate more precise predications than those for the intermetallic size. Also, among the six SFs, the $CPSF^{SY}$ had the lowest S value of 0.0324 with the highest R^2 of 0.9971, which should give the most accuracy in prediction of sludge yield in Mg alloys.

Fig. 11 illustrates the comparison of predicted sludge yields and intermetallic sizes with the experimental measurements for the confirmation experiment with the least sludge formation. For the confirmation experiment with the most sludge formation, the predicted sludge yields and intermetallic sizes were compared with the experimental measurements in Fig. 12. In both Figs. 11 and 12, CSFSY, PSFSY, CPSFSY, CSFIS, PSFIS, and CPSFIS stand for the sludge factors of CSF^{SY}, PSF^{SY}, $CPSF^{SY}$, CSF^{IS}, PSF^{IS}, and $CPSF^{IS}$, while Exp. SY and Exp. IS representing the experimental measurements of the sludge yield and intermetallic size, respectively. In the least sludge cases, the predicted sludge yield of 0.50 wt.% and intermetallic size of 14.66 μm by PSF^{SY} and PSF^{IS} were deviated significantly from the experimental counterparts of 0.26 wt.% and 12.22 μm. Meanwhile, the CSF^{SY}, $CPSF^{SY}$, CSF^{IS}, and $CPSF^{IS}$ computed the sludge yields of 0.35 and 0.34 wt.% and intermetallic sizes of 13.02 and 12.81, which were very close to the measured data of 0.26 wt.% and 12.22 μm. For the most sludge case, the measured sludge yield and intermetallic size were of 0.65 wt.% and 16.02 μm, respectively. The predicted sludge yields and intermetallic sizes by CSF^{SY}, PSF^{SY}, $CPSF^{SY}$, CSF^{IS}, PSF^{IS}, and $CPSF^{IS}$ were 0.64, 0.48 and 0.63 wt.%, and 16.32, 14.39 and 15.95 μm, respectively. The comparison of predicted sludge yields and intermetallic sizes with the experimental measurements indicated that the $CPSF^{SY}$ and $CPSF^{IS}$ gave high accuracy in prediction, as the prediction of the PSF^{SY} and PSF^{IS} had a relatively large deviation from the experimental data. Based on the comparisons made for both the cases, the sludge yields and intermetallic sizes predicted by the CSF^{SY} and CSF^{IS} showed a good fit to the experimental data. Furthermore, the prediction by the $CPSF^{SY}$ and $CPSF^{IS}$ was improved over those of the CSF^{SY} and CSF^{IS}. Their predicted results were in excellent agreement with the experimentally measured sludge yield and intermetallic size, although the $CPSF^{SY}$ and $CPSF^{IS}$ models with five independent variables including both chemical elements and process parameters were more complicated than those of the CSF^{SY} and CSF^{IS} with only three chemistry-related independent variables.

The statistical analysis based on the regression coefficients and the standard error of the regression validated the accuracy of the established Sludge Factors for prediction of sludge yields and intermetallic sizes in Al-containing Mg alloys.

3.1. Sludge formation and particle settling

The previous studies on die cast Al-containing Mg alloys showed that the chemical compositions, holding temperature and times affected the sludge yield and particle size [1–3]. The Mn content in the alloy played a dominant role in sludge formation. The particle size and sludge yield increased with increasing the Mn content in the alloy. Meanwhile, the low temperature and long holding time encouraged the precipitation and coarsening of Mn-rich particles.

It was proposed that the settling velocity of Mn-rich particles could be determined by Stokes' law:

$$\boldsymbol{V_s} = \frac{(\boldsymbol{d_p} - \boldsymbol{d_l})\ \boldsymbol{g}\ \boldsymbol{D_p}}{18\ \eta_l} \tag{25}$$

where V_s is the settling velocity of Mn-rich particles, d_p and d_l are the densities of Mn-rich particles and liquid Mg alloy, respectively, g is the gravitational acceleration (9.806 m^2/s), and η_l is the dynamic viscosity of liquid Mg alloy. Stokes' law considers only individual smooth and spherical solid particles in liquid laminar flow. Since the identified particles in Mg sludge were non-spherical and in irregular shapes, the direct application of Stokes' law could lead to an overestimation of settling velocities. Peng et al. [1] introduced a correction factor and a shape factor into Stokes' law, which overcame its overestimation. With the corrected Stokes' law, the settling speeds of the Al-Mn(-Fe) particles in commercial Mg AZ91 alloy were successfully correlated to the particle sizes. The theoretical settling velocities of the particles as a function of the temperatures and the particle diameters were calculated. The data provided in reference 1 indicated that,

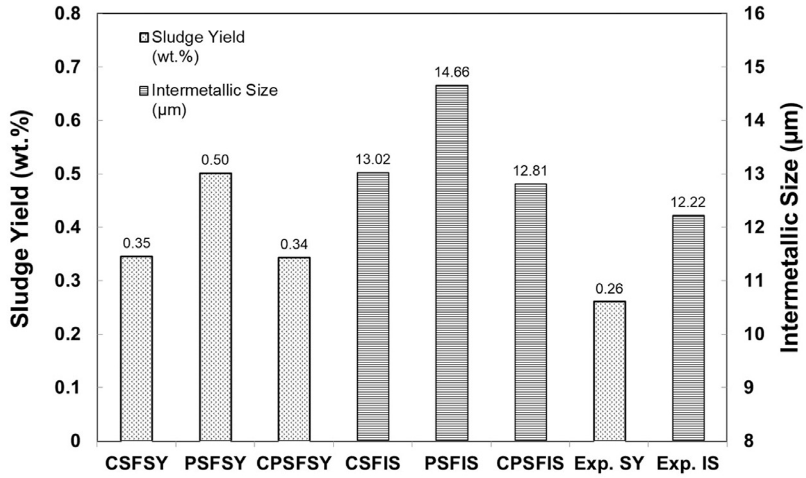

Fig. 11. Comparison of predicted sludge yields and intermetallic sizes with the experimental measurements for the confirmation experiment with the least sludge formation.

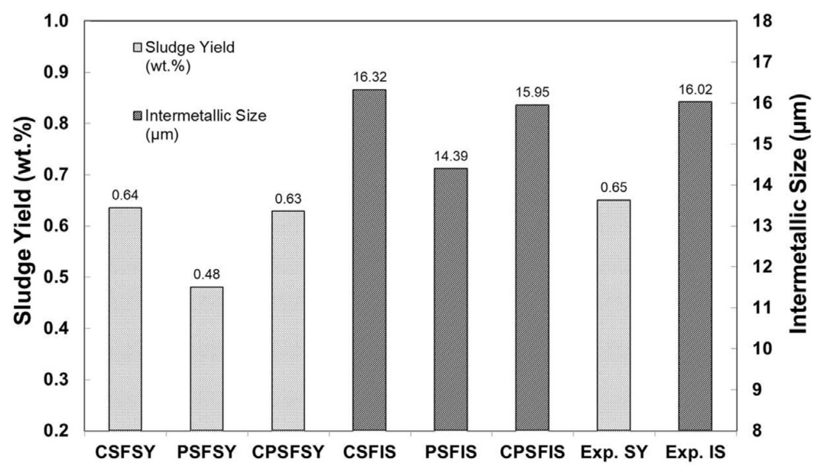

Fig. 12. Comparison of predicted sludge yields and intermetallic sizes with the experimental measurements for the confirmation experiment with the most sludge formation.

when the particles were large at a fixed holding temperature, their settling speeds were high. As the holding temperature decreased for particles with a fixed size, the settling speeds reduced. Hence, to minimize the sludge formation, the holding temperature should be high, while the setting speed and the holding time had to be low and short respectively. The findings of the present studies are consistent with the published results. To quantitatively compute the settling velocities of the Al-Mn particles in the test Mg-Al alloys, the dynamic viscosities and density of the alloys need to be determined.

4. Conclusions

To control the intermetallic formation in the sludge of magnesium alloys, the Design of Experiment based on the Taguchi method was employed to systematically study the effects of chemical compositions and process parameters on the yield and the intermetallic size particles in the sludge of magnesium alloys. The conclusions drawn from this study are given below:

1. Among the selected five factors, Al, Mn and Fe contents as well as holding temperatures and times, Mn was found to be the most influencing factor (91.91%) for the sludge yield, as the other factors had a similar, but much smaller effect on the yield with the Al, Fe, holding temperatures and time contributions of 3.32%, 2.22%, 1.88% and 0.66%, respectively.
2. On the intermetallic size, the holding temperature made the major effect of 33.52% and both the Al and Mn contents had the moderate influences of 27.41% and 27.65%, while the Fe content and holding time contributed only 1.97% and 9.44%, respectively.

3. To achieve the least sludge yield, i.e., the best performance characteristic, the optimum combination (A4B1C1D4E1) with the maximum S/N ratios was 9 wt.% Al, 0.15 wt.% Mn, 0.001 wt.% Fe, 690 °C as the holding temperature, and 30 min as the holding time.
4. The combination (A2B4C4D2E4) for the worst performance characteristics, i.e., the most sludge yield, was 7 wt.% Al, 0.45 wt.% Mn, 0.01 wt.% Fe, 650 °C as the holding temperature, and 120 min as the holding time.
5. For the intermetallic sizes, the combination (A4 B1C1D1E2, i.e., 9 wt.% Al, 0.15 wt.% Mn, 0.001 wt.% Fe, 630 °C as the holding temperature, and 60 min as the holding time, resulted in the smallest intermetallic size. However, the largest intermetallic size was produced by the combination (A2B4C4D3E4) of 7 wt.% Al, 0.45 wt.% Mn, 0.01 wt.% Fe, and 670 °C as the holding temperature, and 120 min as the holding time.
6. To build a Sludge Factor for Mg alloys, multivariate linear regression analyses were carried out with the DOE results. Six Sludge Factor equations for the sludge yield and intermetallic size were established as a function of the chemical compositions and/or the processing parameters.
7. The comparison of the sludge yields and intermetallic sizes predicted by the SFs with the experimental measurements indicated that the Comprehensive Sludge Factor (CPSF) with five independent variables including both chemical elements and process parameters gave high accuracy in prediction, as the prediction of the Process Sludge Factor (PSF) with only the two processing parameters of the melt holding temperature and time showed a relatively large deviation from the experimental data.
8. The Chemical Sludge Factor was primarily designed for small ingot producers and die casters with a limited melting and holding capacity, of which process parameters could be fixed easily. The Physical Sludge Factor could be used for mass production with a single type of Mg alloy, in which the chemistry fluctuation might be negligible. In large Mg casting suppliers with multiple melting and holding furnaces and a number of Mg alloys in production, the Comprehensive Sludge Factor should be implemented to diminish the sludge formation.
9. The established Sludge Factors enable engineers to predict the sludge yield and intermetallic size in Mg alloys during die casting, and to cost-effectively design process parameters with known chemical compositions. To minimize the sludge formation, the SFs can be used as a control measure for the avoidance of sludge buildup in holding crucibles, hard spots in cast components, reduced fluidity of liquid metal to flow into a die.
10. The findings of this work provide valuable tools to control the intermetallic formation in magnesium alloys. They have the potential to enhance casting quality, diminish sludge generation, minimize industrial waste sent to landfills, and ultimately contribute to a reduced environmental impact.

Declaration of competing interest

The authors declare that they have no known competing financial interests or personal relationships that could have appeared to influence the work reported in this paper.

CRediT authorship contribution statement

Y. Fu: Writing – review & editing, Writing – original draft, Visualization, Validation, Investigation, Formal analysis, Data curation. **G.G. Wang:** Writing – review & editing, Supervision, Project administration, Methodology, Funding acquisition, Conceptualization. **A. Hu:** Writing – review & editing, Writing – original draft, Methodology, Investigation, Conceptualization. **Y. Li:** Writing – review & editing, Writing – original draft, Methodology, Investigation, Conceptualization. **K.B. Thacker:** Project administration, Investigation, Conceptualization. **J.P. Weiler:** Writing – review & editing, Writing – original draft, Project administration, Methodology, Investigation, Funding acquisition, Formal analysis, Conceptualization. **H. Hu:** Writing – review & editing, Writing – original draft, Validation, Supervision, Resources, Project administration, Methodology, Investigation, Formal analysis, Data curation, Conceptualization.

Acknowledgments

The authors would like to thank the Meridian Lightweight Technologies Inc., Strathroy, Ontario Canada, and the University of Windsor, Windsor, Ontario, Canada for supporting this work. This work is part of a large project funded by Meridian Lightweight Technologies, Inc.

References

[1] L. Peng, G. Zeng, T.C. Su, H. Yasuda, K. Nogita, C.M. Gourlay, JOM 71 (7) (2019) 2235–2243.
[2] G. Zeng, J.W. Xian, C.M. Gourlay, Acta Mater. 153 (2018) 364–376.
[3] Y. Fu, G. Wang, A. Hu, Y. Li, K.B. Thacker, J.P. Weiler, H. Hu, J. Magnes. Alloys 10 (3) (2022) 599–613.
[4] A. Thorvaldsen, N. Fantetti, C.A. Aliravci, in: Extraction, Refining, and Fabrication of Light Metals, Pergamon, 1991, pp. 413–421.
[5] O. Holta, H. Westengen, J. Roen, in: Proceeding of the 3rd International Magnesium Conference, Manchester, United Kingdom, UMIST, 1997, pp. 75–87.
[6] O. Holta, H. Westengen, in: Proceedings of the International Symposium on Advanced Transportation Applications, Aachen, 1994 94NMO42.
[7] C.P. Corby, N. Ricketts, M. Qian, R.D. Bailey, Magnes. Technol. (2004) 209–214.
[8] H.Z. Ye, X.Y. Liu, J. Alloys Compd. 419 (1–2) (2006) 54–60.
[9] S.L. Sin, A. Elsayed, C. Ravindran, Int. Mater. Rev. 58 (7) (2013) 419–436.
[10] J.M. Tartaglia, J.H. Howard, R.E. Swartz, R.L.J. Bentz, JOM 53 (11) (2001) 16–19.
[11] H. Hu, A. Luo, JOM 48 (1996) 47–51.
[12] A.G. Haerle, B.A. Mikucki, W.E. Mercer II, Light Met. Age 54 (1996) 22–29.

[13] M. Paradis, A.M. Samuel, H.W. Doty, F.H. Samuel, Int. J. Met. Cast. 12 (2018) 2–19.
[14] P. Bakke, G.G. Wang, D. Albright, NADCA Trans. (2001) T01- 061.
[15] P. Bakke, D.O. Karlsen, J. Mater. Manuf. 106 (1997) 314–326.
[16] B. Bronfin, N. Polyak, E. Aghion, C. Fuerst, D. Barris, in: Proceedings of the Magnesium Technology 2002 Symposium, Seattle, WA, USA, TMS, 2002, pp. 55–60.
[17] B. Bronfin, N. Moscovitch, Met. Sci. Heat Treat., 48 (2006) 479–486.
[18] J.L. Jorstad, Die Cast. Eng. 30 (6) (1986) 1–6.
[19] D.E. Groteke, Die Cast. Eng. 5 (29) (1985) 16–24.
[20] S.G. Shabestari, J.E. Gruzleski, Cast Met. 6 (4) (1994) 217–224.
[21] A. Flores, J.C. Escobedo, M. Mendez, J. Mendez, in: Proceedings of the Transactions of International Die Casting Congress and Exposition, Drtroit, Michigan, USA, 1991, pp. 293–297. Sept. 30 – Oct. 3.
[22] M.M. Makhlouf, D. Apelian, Casting Characteristics of Aluminum Die Casting Alloys, Worcester Polytechnic Institute, Worcester, Massachusetts, USA, 2002 DOE report(No. DOE/ID/13716).
[23] R. Beygi, I. Galvão, A. Akhavan-Safar, H. Pouraliakbar, V. Fallah, L.F.M. da Silva, Metals 13 (2023) 768.
[24] R. Beygi, H. Pouraliakbar, K. Torabi, G. Eisaabadi B, V. Fallah, S.K. Kim, R. Shi, L.F.M. da Silva, J. Manuf. Process. 70 (2021) 152–162.
[25] H. Pouraliakbar, Z. Ghorbanzadeh, V. Fallah, Mater. Lett. 355 (2024) 135548.
[26] Z. Ghorbanzadeh, H. Pouraliakbar, V. Fallah, J. Alloys Compd. 969 (2023) 172477.
[27] G. Taguchi, Introduction to Quality Engineering, McGraw-Hill, New York, 1986.
[28] Z. Sun, H. Hu, X. Chen, J. Mater. Process. Technol. 199 (2008) 256–264.
[29] L.M. Chihara, T.C. Hesterberg, in: Mathematical Statistics with Resampling and R, 2nd ed., John Wiley & Sons, 2019, pp. 297–358.